

# Stationary surface waves and antidunes in dense pyroclastic density currents

5 Pete Rowley<sup>1</sup>, Guido Giordano\*<sup>2</sup>, Aurora Silleni<sup>2,3</sup>, Greg M Smith<sup>4</sup>, Matteo Trolese<sup>2</sup> and Rebeca Williams<sup>4</sup>

<sup>1</sup> School of Earth Sciences, University of Bristol, Bristol, UK

<sup>2</sup> Dipartimento di Scienze – Sezione Geologia, Università di Roma Tre, Roma, Italy

<sup>3</sup> Università degli studi di Napoli Federico II, Italy

10 <sup>4</sup> School of Environmental Sciences, University of Hull, UK

Corresponding author: [pete.rowley@bristol.ac.uk](mailto:pete.rowley@bristol.ac.uk)

15

This manuscript has not undergone peer review. It has been submitted for publication at Volcanica.

20 Subsequent versions may have slightly different content. If accepted, the final version of this manuscript will be available via the “Peer reviewed publication DOI” link to the right on the website. We welcome comments or questions.

# Stationary surface waves and antidunes in dense pyroclastic density currents

30 Pete Rowley\*<sup>1</sup>, Guido Giordano<sup>2</sup>, Aurora Silleni<sup>2</sup>, Greg M Smith<sup>3</sup>, Matteo Trolese<sup>2,4</sup> and  
Rebecca Williams<sup>3</sup>

<sup>1</sup> School of Earth Sciences, University of Bristol, Bristol, UK


<sup>2</sup> Dipartimento di Scienze – Sezione Geologia, Università di Roma Tre, Roma, Italy


<sup>3</sup> School of Environmental Sciences, University of Hull, UK

<sup>4</sup> Istituto Nazionale di Geofisica e Vulcanologia, Pisa, Italy

35 \* pete.rowley@bristol.ac.uk [corresponding author]

 ORCID (FA): 0000-0002-8322-5808

 ORCID (SA): 0000-0002-5819-443X

 ORCID (TA): 0000-0002-5675-072X

40 ORCID: 0000-0003-4192-3170

ORCID: 0000-0003-4356-4132

ORCID: 0000-0002-8203-9982

**Keywords:** antidunes; dense granular; stationary wave; pyroclastic density current; critical flow

## Abstract

45 Stationary antidunes are a product of critical flow in open channel systems, but with poor preservation potential. They are related to the existence of stationary surface waves in the overriding current, but their existence in the dense pyroclastic density current regime has been unrecognized to date. Experiments presented here demonstrate that surface waves in simulated dense pyroclastic density currents show both supercritical downstream-migrating and critical stationary wave behaviour.

50 Deposits from the Pozzolane Rosse ignimbrite (Italy) demonstrate the presence of stationary wave antidunes in deposits from dense pyroclastic currents which imply progressive aggradation from long-lived quasi-stable critical flow conditions during their emplacement. The narrow stability fields for the formation of these deposits reinforces that they are unlikely to be widely preserved in the geological record, but highlights that dense pyroclastic density currents cannot be assumed to be simply

55 supercritical flows, and they may be substantially slower than over-riding dilute currents.

## Introduction

60 Pyroclastic density currents (PDCs) are a widespread and hazardous phenomenon at active volcanic centers around the world (Brown et al., 2017; Wilson et al., 2014). They are heterogenous and often highly mobile multi-phase currents, comprised largely of juvenile tephra and exsolved and entrained gases. The deposits from these currents often contain a range of sedimentary features which can provide a window to interpret flow conditions during the emplacement of the deposit (Brown, 2017; Douillet et al., 2013; Smith et al., 2020; Smith & Kokelaar, 2013).

65

PDCs are temporally and spatially variable in their structure, and can comprise both dense granular and dilute turbulent regimes (Branney & Kokelaar, 1997, 2002). Mobility of PDCs is often very high, which is largely attributed to the rate of mass exchange between the turbulent and dilute transport system and its dense granular basal current (Shimizu et al., 2019). In currents which support a dense granular basal layer, depositional lithofacies must reflect the emplacement dynamics of that layer, where gas fluidization reduces particle interactions, and hence the internal friction of the current (Sparks, 1976; Wilson, 1980; Druitt *et al.*, 2007, Lube et al 2019). Assuming that dense granular regimes are common in the undercurrents of ignimbrite-forming PDCs (Giordano & Cas, 2021), deposits must commonly form at the flow boundary zone of a dense granular flow base. However, due to the opaque over-riding turbulent flow, and the destructive nature of PDCs, we have no in-situ measurement or observations of the behaviour of these dense basal currents in the field.

80 The criticality of the dilute regime, and the bedform growth processes therein are hotly debated (Douillet, 2021). The presence of bedforms described as antidunes in these dilute conditions have variously been ascribed to supercritical flow (Brand & Clarke, 2012; Fisher et al., 1983; Moorhouse & White, 2016; Schminke et al., 1973), local flow reversals (Andrews & Manga, 2012), or subcritical lower flow regime conditions (Sohn & Chough, 1993) due to their often steep forms, while field observations have identified single bedforms with a character typifying both sub- and super-critical nature (Douillet et al., 2013, 2018).

85

The growth of bedforms in the deposits of experimental supercritical dense granular currents and from PDCs with similar scaled properties have been documented (Lube et al., 2011; Pollock et al., 2019; Rowley et al., 2011; Smith et al., 2020), and a growing catalogue of tools now exists to begin to infer flow conditions within natural PDCs. The bedforms we explore here are morphologically similar to

90 some of the antidunes described in dilute flow deposits, but from unequivocally dense currents, and  
using flume experiments in which we can calculate Froude numbers to determine criticality. In this work  
we explore surface wave behaviours in flowing and sedimenting granular currents to address (1) the  
potential for surface waves in these currents to control depositional behaviour, (2) the occurrence of  
these sedimentary features in the geological record, and (3) what constraints these might place on  
95 interpreting current properties from deposits.

## Method

Experimental work was based on the method developed in Rowley *et al.* (2014), and conducted using  
the flume apparatus described in full by Smith *et al.*, (2018), which has the capability to provide varying  
100 gas fluidisation to over-riding granular currents (Figure 1). This 3 m long flume has a width of 150 mm,  
and mass flux ranging between 0-20 kg/s. 45-90 micron silica lime ballotini were used as the bulk of  
the material, with a 10% by mass doping of 200 micron diameter black beads of the same specific  
gravity. These act as effective tracking markers for interpretation of high speed video footage. Using  
oblique illumination and a top-down camera location we were able to capture the formation and  
105 migration of surface waves.

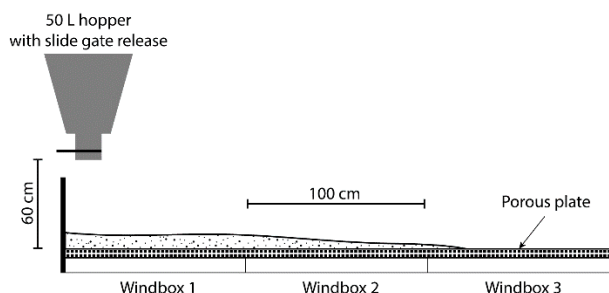


**Figure 1. Flume apparatus, showing the three windboxes each supplied with an independent dried compressed air supply, sitting below a continuous porous plate. This enables the overpassing current to be gas fluidized, or allowed to defluidise at a controlled rate.**

110 5 kg of material was released in each experiment at a mass flux of 10 kg/s. The current which was  
generated was fully fluidized for the first 1 m of propagation as a gas supply above the minimum  
fluidization velocity ( $U_{mf}$ ) was supplied. The currents then transition to a second 1 m section of flume,  
where a gas supply of between 0.6 and 1.0  $U_{mf}$  was supplied (“aerated” conditions, Smith *et al.*, 2018),  
in order to enable deposition while encouraging sufficient propagation for the surface waveforms to

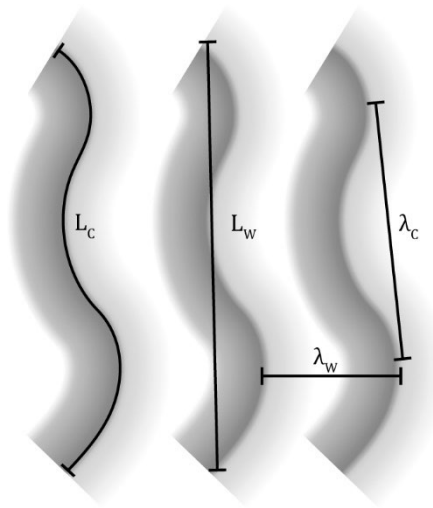
115 develop. The current heads came to a halt at between 1.3 and 1.5 m runout.

All observations in this work focus on the region of the flume between 100 – 130 cm from the start of the flume, which is the critical window in which the current is allowed to defluidise and deposit. Analysis was conducted using manual frame-by-frame tracking of marker particles, and of topographic features  
120 illuminated by the low-angle lighting.

The current velocity is measured using the passage of the tracking particles, while the velocity of the surface waves is measured by tracking their crests as illuminated by the oblique lighting. Surface wave morphology is described using several metrics outlined in Figure 2, and the calculated wave sinuosity  
125 (S) using the straight-line and curvilinear crest lengths ( $L_S$  and  $L_C$  respectively):

$$S = \frac{L_C}{L_S}$$

where a perfectly straight wave will result in  $S=1$ , with greater values indicating higher sinuosity.



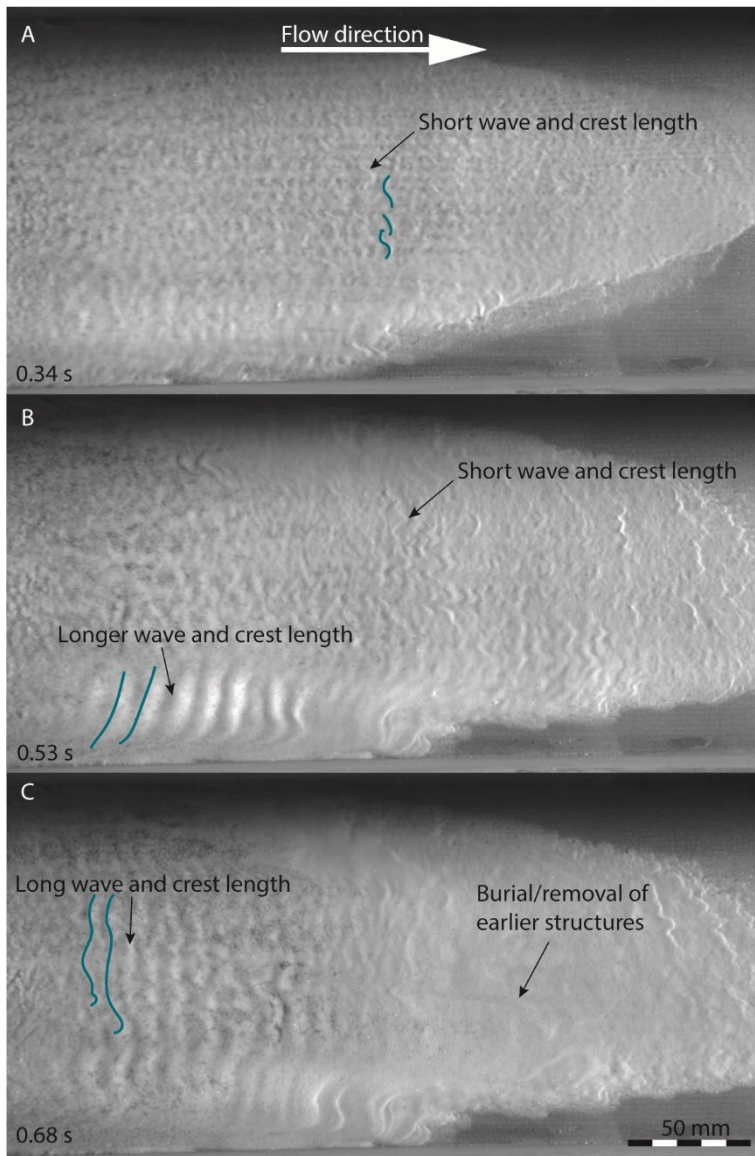
130 **Figure 2. Morphometric parameters describing the surface waves, establishing the distance between subsequent surface waves (surface wave wavelength,  $\lambda_w$ ), the wavelength of irregularity in the surface wave crest (crest wavelength,  $\lambda_c$ ), the total curvilinear length following the crest of a surface wave (curvilinear length,  $L_C$ ), and the straight-line length between each end of the wave (straight-line length,  $L_S$ ) is the.**

## Results

135 As the fully fluidised current transitions into the aerated section of the flume (where 0.6, 0.9, or 1  $U_{mf}$  is  
being supplied) it gradually decelerates, and comes to a halt (see supplementary video files 1-3). The  
higher gas flow rates lead to slower defluidisation and loss of aeration, and are related to higher  
mobility. As the current velocity drops the rate of deceleration increases, indicating the frictional  
jamming of the granular particles as the material defluidises. The side walls, then current front are the  
140 first part to come to rest.

The current head is initially dominated by thin surging current packages, which propagate at around  
0.8 - 1 m/s. This early phase of the current shows longitudinal string-like features which are likely the  
result of defluidisation bubble trains, as these very thin current heads degas.

145  
During the deceleration of the currents a population of surface waves evolve through time and space  
from small, chaotically-arranged high-sinuosity waves to larger, longer wavelength and less sinuous  
waves (Figure 3). The first surface waves appear at relatively high current velocities of  $\sim 1$  m/s (Figure  
4A), and they remain present until the current has nearly come to a halt. These typically travel  
150 downstream at a velocity approaching that of the current itself. Through time the surface waves evolve  
into larger long-wavelength less sinuous surface waves, which have a lower velocity relative to the  
flume bed. Current velocity at a point is a poor predictor of co-located surface wave morphology  
(Figure 4B, 4C), and fluidisation state is not a controlling factor in any of the investigated parameters.



155 **Figure 3. Three frames of high speed video from the  $0.6 U_{mf}$  experiment, showing the upper surface of a current propagating left to right. High sinuosity short wavelength surface waves develop early in the shallow current [A], with larger and longer wavelength surface waves developing later as the current thickens [B, C]. Some example wave crests have been picked out in each frame. As the flow comes to a halt the waves are buried or lost [C].**

160

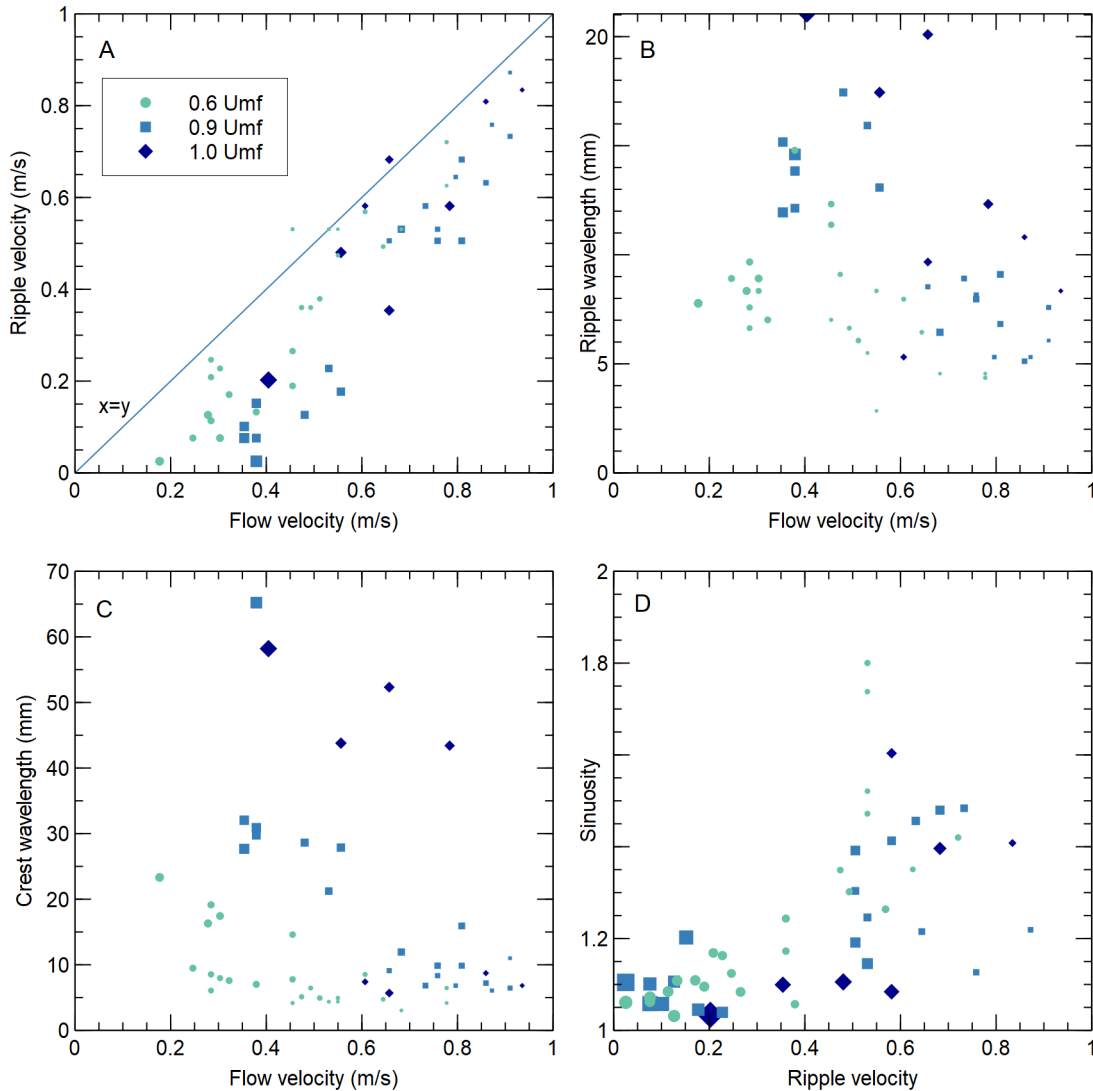


**Figure 4. Velocity and morphology relationships across the range of fluidisation states investigated (circle  $0.6 U_{mf}$ , square  $0.9 U_{mf}$ , diamond  $1.0 U_{mf}$ ). Symbols are scaled with time, with smaller symbols representing data early in the currents propagation, and the largest representing 1.2 seconds from the current entering the video frame. Wave velocity varies with (and is limited by) current velocity.**

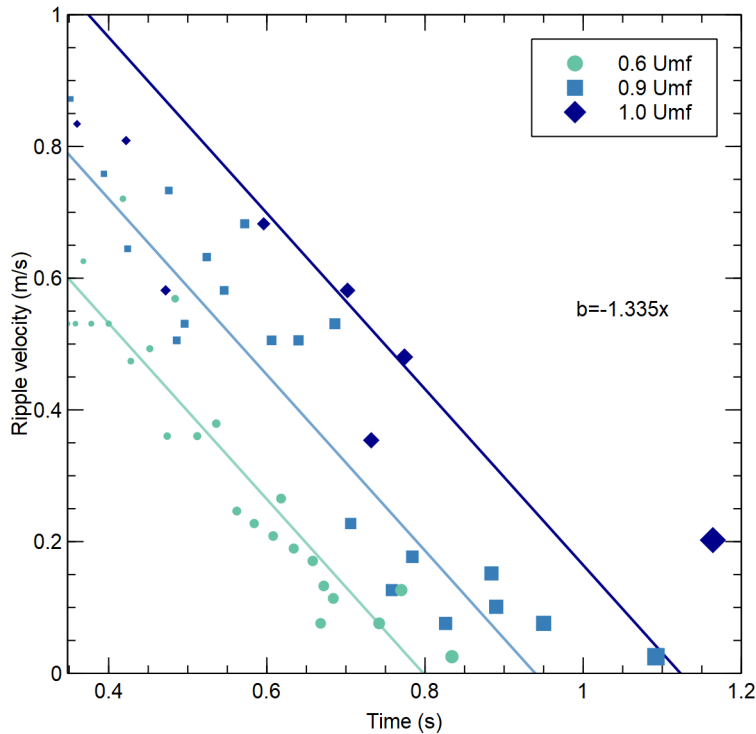
165

The depletive waning nature of these currents causes a thickening of the current as it develops. The apparatus is not capable of resolving current thickness at the resolution necessary to be meaningful for this work. However, time can be used as a proxy for the developing thickness of the current as it slows

170 (Figure 5). This produces very consistent fits for the surface wave velocity data, suggesting that the

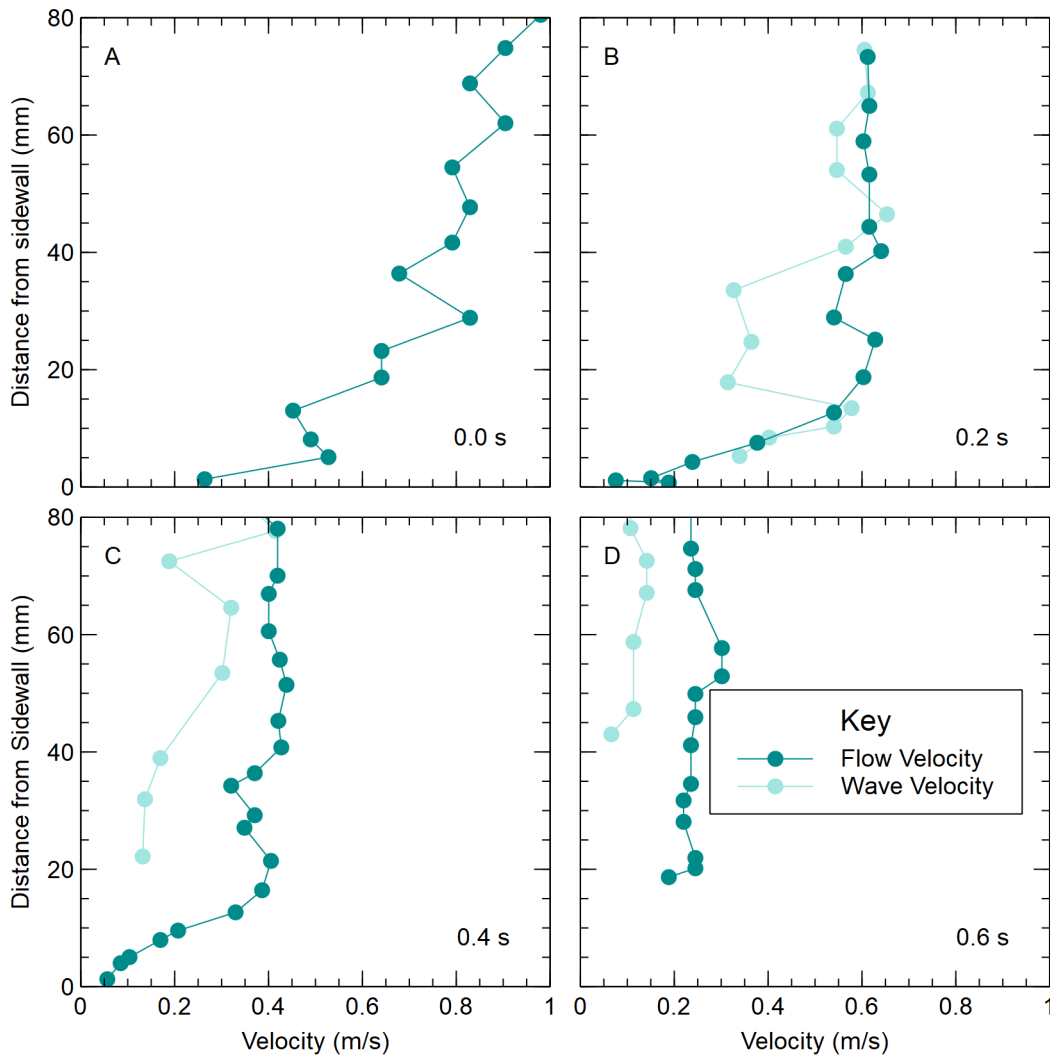


noise seen in the earlier (Fig 4A) plots might be explained by a thickness dependence, rather than simply current velocity.



175 **Figure 5. Surface wave velocity as a function of time, showing a linear relationship. Note that the X-axis offset between the three suites of data is a product of the higher entry velocity of the more fluidised currents. However, they track the same linear relationship with a gradient of -1.335.**

It is evident from the video frames (Figure 3) that the experiment is impacted by sidewall friction. We can explore temporal changes in the cross-channel behaviour of the current using this footage, which  
 180 can inform us about the surface wave development further. Tracking current and wave velocities at 0.2 second intervals in a single experiment, and plotting these relative to the distance from the sidewall (Figure 6), it is immediately apparent that the current velocities have a higher magnitude in the centre of the flume than at the sidewall. As the current develops and slows, the sidewalls come to a halt first. These plots reinforce the observations from Figure 4A, that as the current velocity falls below 0.4 m/s  
 185 the surface waves become near stationary relative to the bed (wave velocity,  $U_w = 0$ ). These near-stationary waves can be seen in the supplemental video files provided.



190 **Figure 6. Velocity of current (dark) and waves (pale) at 0.2 second intervals following the passage of the current front [A-D] in a weakly aerated current ( $0.6 U_{mf}$ ). The current is noticeably slowed by sidewall interactions throughout, with the sidewall having come to a halt within 0.5 seconds of the current front passing.**

## Discussion

The relationship between wave and current velocity for these experiments closely follows a straightforward positive linear correlation with a gradient of 1, but an X intercept of approximately 0.2 m/s (Figure 4A). There are hints that this intercept increase with  $U_{mf}$ , but this will require further work to

195

demonstrate. More interesting is that this relationship is maintained for different fluidisation conditions, which is a primary control on velocity. Given the time dependence of velocity in these depletive currents, and the correlating change in current thickness, it is likely that current thickness is exerting a control on wave propagation. However, our existing apparatus does not permit us to interrogate this directly. Sidewall observations suggest the flowing region in these currents varies between <1 – 10 mm thickness, with a thin current head which thickens through time before the current comes to a halt. If future work can quantify thickness effectively, then this would suggest that sedimentary structures which inform of the current criticality, or which capture sinuosity or wavelength data, would be able to provide information on the original current conditions.

205

While a strict stationary-wave situation does not appear to have been achieved here (recorded wave velocities reach 0.02 m/s before burial), the data suggest this is a possible scenario in these current conditions. Furthermore, if we assume that stationary waves require a Froude Number (Fr) of ~1 (as per hydraulic flow) then we can begin to use stationary wave formation to understand the current.

210

$$Fr = \frac{U_f}{\sqrt{gh}} \quad (1)$$

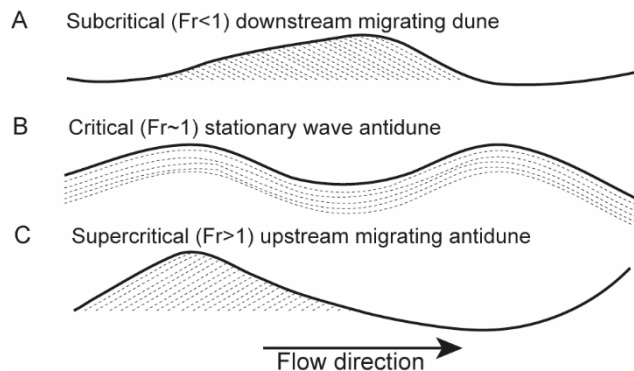
Where  $U_f$  is current velocity,  $g$  is acceleration due to gravity, and  $h$  is current thickness. Indeed, in the case presented here, with  $h$  in the order of <1 cm, Fr drops from over 20 at the current front to ~1 as our wave velocity approaches 0.

215 This critical flow condition is difficult to achieve in laboratory experiments, due to the defluidisation timescales of the materials being used; the currents suffer from frictional slowing and compaction before they are able to enter a stable critical or subcritical flow condition. However, larger natural currents experience slower degassing (Druitt et al., 2007) and therefore may have the potential to capture more stable and long-lived stationary wave sedimentary behaviours.

220

In hydraulic currents stationary waves are typified by in-phase antidune formation (Figure 7), with either downslope or upslope migration as the flow alternates between  $Fr < 1$  and  $Fr > 1$  conditions, respectively (Kennedy, 1963). Similar features have been recorded in ignimbrites, although the cross bedding is often difficult to observe due to the very poorly sorted nature of the deposit, rarely ideal

225 section angles, and loss of preservation due to waxing and waning flow, and the resulting erosion and  
resedimentation of material under highly varying conditions. However, examination of the Pozzolane  
Rosse ignimbrite, deposited by eruption from Colli Albani (Italy) shows an exemplary sequence of  
stationary wave antidunes, which preserve sequential growth of a 10+ m thick sediment pile which we  
interpret to capture sustained flow and deposition at or around  $Fr=1$ .



230

**Figure 7.** Dune forms related to [A] subcritical, [B] critical and [C] supercritical conditions as recognised in hydraulic currents.

### Application to the Pozzolane Rosse

The Pozzolane Rosse is a somewhat unusual ignimbrite, in that it is fines depleted, and of a relatively  
dense juvenile material (Giordano *et al.*, 2010; Trolese *et al.*, 2017; Smith *et al.*, 2020; Calabrò *et al.*  
235 2022). It is the deposit of a widespread PDC erupted from Colli Albani volcano (Italy), around  $456 \pm 3$   
ka (Marra *et al.*, 2009). The deposits investigated here focus on the Eastern sector of the volcano,  
approximately 25 km from the source vent.

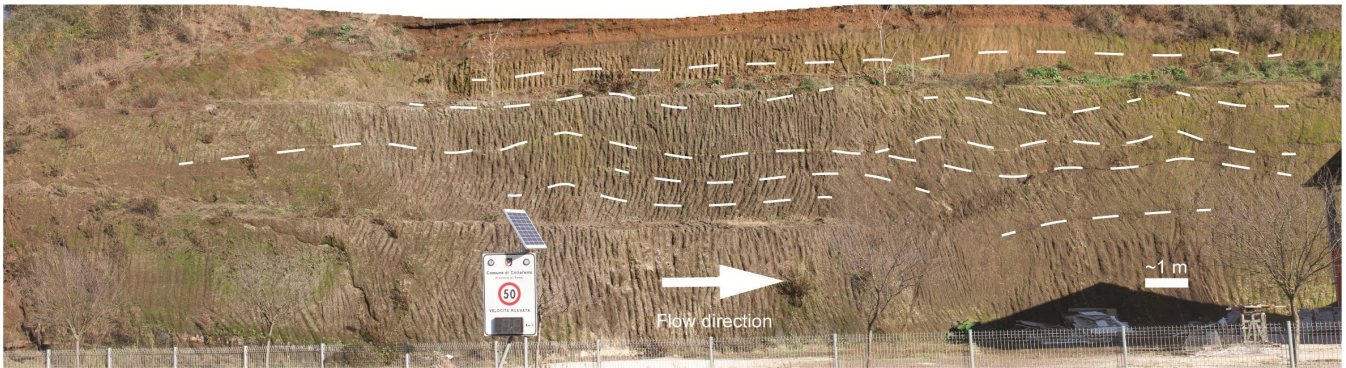
240 A large 3D exposure at Colleferro Scalo (41.7442 N, 13.0026 E) reveals a sequence of dune forms  
deposited by a current flowing SE from Colli Albani. These beds allow us to interpret the development  
of a current in three stages. There is an initial sequence which shows in-phase antidunes with a crest-  
to-crest wavelength of approximately 3 m, and amplitudes in the order of 0.5-1 m (lower two beds, blue  
dotted line in Figure 8A). These transition to short ( $< 0.5$  m) sequences of out-of-phase bedforms,  
245 perhaps indicating waxing or waning of the flow (upper beds in white dashed lines in Fig. 8A). The  
deposit then transitions upward building a sequence of identifiable in-phase horizons, each  $\sim 1-4$  m

thick, with crest-to-crest wavelengths in the order of 10 m and amplitudes on the order of 1 m (red dotted lines in Figure 8B).



250 **Figure 8. Exposure of (A) alternating in- and out-of-phase bedforms in an aggrading sequence of the**  
**Pozzolane Rosse ignimbrite, transitioning upward into (B) a ~8 m thick stable sequence of in-phase**  
**bedforms. Bed interfaces picked out in blue dots for the lower in-phase antidunes, red dots for the**  
**upper in-phase antidunes, and white dashed lines for out of phase or unclear beds. Black dashed**  
**line indicates corner of quarry face with ~90 degree return, giving a 3D section. Note that panel A**  
255 **connects to the lower left of panel B. 41.7442 N, 13.0026 E, looking NE (A) and E (B). Un-annotated**  
**imagery is provided in the supplemental file 4.**

Approximately 300 m WNW (Upstream) of this position at 41.7453 N, 12.9973 E, a terraced section to  
the North East of the road exposes a similar series of bedforms (Figure 9). Here there are crest-to-  
crest wavelengths ranging between 3 and 10 m, and similar amplitudes of 0.5-1 m. Assuming the  
260 wavelength properties of the bedforms are representative of flow conditions, and that the deposit seen  
here is indeed synchronous with that seen in Figure 8 (which is a reasonable assumption on the  
locations altitudes, and bed dips), these suggest that flow conditions in this area were similar over  
distances in the order of >300 m, and for durations capable of sedimenting up to 10 m of material.



265 **Figure 9. Cut terraced section of Pozzolane Rosse ignimbrite, with flow from left to right, bed interfaces picked out in white. 41.74424 N, 13.0026 E, looking NE. An un-annotated version of this figure is provided in the supplementary file 5.**

Uniform sedimentation across these bedforms from a unidirectional PDC suggests that the current was remarkably in steady-state for a period of at least minutes, and throughout this time was aggrading a deposit through relatively uniform deposition. This implies there were not any substantial thalwegs of current migrating across this area during this time, so quasi-steady conditions were able to exist. Relatedly, this implies that the eruption feeding the current was also steady during this phase. Interestingly, the transverse sections seen in Figure 8B suggest that toward the top of the sequence thalwegs may have started to develop, as we see a central levee/bank develop towards the top of the sequence. This might suggest that in later stages of this current the steadiness broke down.

While experimental work has begun to establish stability conditions for backset bedforms and instability features (Smith et al., 2020), there is not yet sufficient data to begin to use these dune morphologies to estimate flow properties here. However, given the Froude criticality condition, we can begin to narrow down some of these parameters. Notably, a requirement of  $Fr \sim 1$  places quite tight constraints on  $U_f$ .

For dense-current flow thicknesses of up to 5 m, we find that  $U_f$  cannot exceed 10 m/s, and even for substantially thicker currents, the velocity does not meaningfully increase from this order of magnitude (Figure 10). This is substantially slower than anticipated for most PDCs (Legros & Kelfoun, 2000; Lube, Cronin, et al., 2011; Pollock et al., 2019; Sulpizio et al., 2014).

Given the rarity of finding critical and subcritical conditions in experimental currents, we suggest that the conditions for these slow critical/subcritical currents are rare, and hence the formation of stationary

waves is unusual. The deposits captured in this portion of the Pozzolane Rosse are therefore likely to be an interesting case study, but not representative of widespread ignimbrite conditions. This agrees with the Colferro locality being located just beyond a major sedimentary trap, hence capable of significantly slowing the dense basal current (Giordano and Doronzo 2017). Alternatively, and more interestingly, in the rare case studies where flow velocity derived from ignimbrite features have been proposed, velocities in the range of 10 m/s (Pittari et al. 2006; Cas et al. 2011; Roche et al. 2016) are found. These low velocity values may be indicative of sedimentation conditions of the dense basal granular current but potentially not of the current velocity of the over-riding dilute and turbulent PDC (Fisher 1995; Branney and Kokelaar 2002. Velocities of the dilute part of the Pozzolane Rosse PDC have been numerically modelled to range between 50-150 m/s at 25 km from vent, i.e. at distances comparable to those of Colferro locality (Calabrò et al. 2022). If the lower deposit velocities in the order of a few meters to tens of meters per second are true, then we must consider that an order of magnitude difference between the dense and dilute flow velocities may be realistic in large volume PDCs, and critically that the deposit will record the conditions in the dense slower current much more easily.

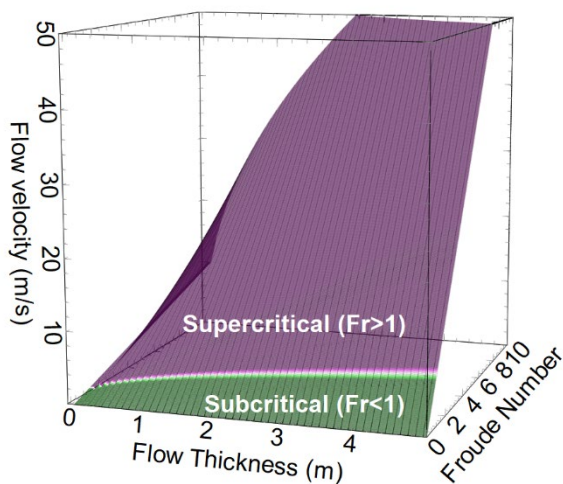


**Figure 10.** Plot of Froude number at given flow velocity vs flow thickness values, demonstrating the narrow criticality field where  $Fr=1$  (white).

## Conclusions

Surface waves in unidirectional granular currents may be an important component in developing bedform features within deposits. Evidence here suggests that stationary waves in granular currents require similar conditions to stationary waves in hydraulic flow (i.e.  $Fr=1$ ). Therefore, stationary waves  
310 may exist, but are unlikely to be a common feature preserved in natural deposits, given the very narrow field of stability for  $Fr=1$  conditions. Surface wave geometry is closely tied to the current velocity and thickness, with increasingly supercritical conditions associated with higher sinuosity, smaller surface wave lengths, and shorter wavelengths between waves.

315 In-phase stationary wave deposits identified in the Pozzolane Rosse are an unusual example, but demonstrate the ability for sustained quasi-steady flow to develop thick deposits through a process of aggradation which captures current behaviours representative of the dense granular regime above. These provide evidence that some bedforms in dense granular PDC may be a product of not solely conditions at the flow boundary zone, but the entire dense layer thickness, its surface waves, and how  
320 these interact with the basal topography.

This work adds to the evidence that basal currents in some large PDCs may be moving at an order of magnitude lower velocities than the over-riding turbulent flow. However, this dense current and its flow boundary zone with the substrate is responsible for the bulk of deposit aggradation (Branney and  
325 Kokelaar 2002, Smith et al 2020). Improving our understanding of flow regimes in the dense undercurrent is therefore the key to understanding PDC deposits, and opens up an exciting opportunity to quantitatively explore the feedback between the dense and dilute part of the PDC (e.g. Breard et al 2016; Shimizu et al. 2019).

330 The work here explores conditions in fine grained unimodal currents at laboratory scale current thicknesses and velocities. Experiments at other scales, and using a wider range of materials are needed in order to expand our understanding of the stability fields to more widely apply this methodology to the interpretation of field deposits.

## 335 **Author contributions**



PR initiated the work, carried out the experimental study, and drafted the manuscript. PR, GG, AS, GS, MT and RW carried out field observation and discussion, contributed to data interpretation, and revision of the manuscript.

## 340 **Acknowledgements**

The experimental work was conducted using equipment purchased under a British Society for Geomorphology Early Career Researcher Grant to PR in 2016. Fieldwork was supported by the University of Hull Doctoral Scholarship awarded to GS under the Catastrophic Flows Research Cluster.

## 345 **Data availability**

Compressed high speed video of the experiments is provided in the supplementary materials, while original frame-by-frame images are available in the following open access repositories. 0.6  $U_{mf}$  image files at DOI:10.5281/zenodo.7766160, 0.9  $U_{mf}$  image files at DOI:10.5281/zenodo.7766183, and 1.0  $U_{mf}$  image files at DOI:10.5281/zenodo.7766576.

350

## **References**

- Andrews, B. J., & Manga, M. (2012). Experimental study of turbulence, sedimentation, and coignimbrite mass partitioning in dilute pyroclastic density currents. *Journal of Volcanology and Geothermal Research*, 225–226, 30–44. <https://doi.org/10.1016/j.jvolgeores.2012.02.011>
- 355 Brand, B. D., & Clarke, A. B. (2012). An unusually energetic basaltic phreatomagmatic eruption: Using deposit characteristics to constrain dilute pyroclastic density current dynamics. *Journal of Volcanology and Geothermal Research*, 243–244, 81–90. <https://doi.org/10.1016/j.jvolgeores.2012.06.011>
- 360 Branney, M. J., & Kokelaar, P. (1997). Giant bed from a sustained catastrophic density current flowing over topography: Acatlán ignimbrite, Mexico. *Geology*, 25(2), 115–118. [https://doi.org/10.1130/0091-7613\(1997\)025<0115:GBFASC>2.3.CO;2](https://doi.org/10.1130/0091-7613(1997)025<0115:GBFASC>2.3.CO;2)
- Branney, M. J., & Kokelaar, P. (2002). Pyroclastic Density Currents and the Sedimentation of Ignimbrites. *Geological Society Memoir*, 27(1). <https://doi.org/10.1144/GSL.MEM.2003.027.01.02>
- 365 Breard, E., Lube, G., Jones, J. et al. Coupling of turbulent and non-turbulent flow regimes within pyroclastic density currents. *Nature Geoscience* 9, 767–771 (2016). <https://doi.org/10.1038/ngeo2794>
- Brown, S. K., Jenkins, S. F., Sparks, R. S. J., Odbert, H., & Auker, M. R. (2017). Volcanic fatalities database: analysis of volcanic threat with distance and victim classification. *Journal of Applied Volcanology*, 6(1). <https://doi.org/10.1186/s13617-017-0067-4>
- 370 Calabrò, L., Esposti Ongaro, T., Giordano, G., & de'Michieli Vitturi, M. (2022). Reconstructing pyroclastic currents' source and flow parameters from deposit characteristics and numerical modeling: The Pozzolane Rosse ignimbrite case study (Colli Albani, Italy). *Journal of Geophysical*

- Research: Solid Earth, 127(5), e2021JB023637. <https://doi.org/10.1029/2021JB023637>
- 375 Cas, R. A. et al. (2011) 'The flow dynamics of an extremely large volume pyroclastic flow, the 2.08-Ma Cerro Galán Ignimbrite, NW Argentina, and comparison with other flow types', *Bulletin of volcanology*, 73, 1583-1609. <https://doi.org/10.1007/s00445-011-0564-y>.
- Douillet, G. A. (2021). The supercritical question for pyroclastic dune bedforms: An overview. *Sedimentology*, 68(4), 1698–1727. <https://doi.org/10.1111/sed.12859>
- 380 Douillet, G. A., Kueppers, U., Mato, C., Chaffaut, Q., Bouysson, M., Reschetizka, R., Hoelscher, I., Witting, P., Hess, K. U., Cerwenka, A., Dingwell, D. B., & Bernard, B. (2018). Revisiting the lacquer peels method with pyroclastic deposits: Sediment plates, a precise, fine scale imaging method and powerful outreach tool. *Journal of Applied Volcanology*, 7(1). <https://doi.org/10.1186/s13617-018-0080-2>
- 385 Douillet, G. A., Pacheco, D. A., Kueppers, U., Letort, J., Tsang-Hin-Sun, È., Bustillos, J., Hall, M., Ramón, P., & Dingwell, D. B. (2013). Dune bedforms produced by dilute pyroclastic density currents from the August 2006 eruption of Tungurahua volcano, Ecuador. *Bulletin of Volcanology*, 75(11), 1–20. <https://doi.org/10.1007/s00445-013-0762-x>
- 390 Druitt, T. H., Avard, G., Bruni, G., Lettieri, P., & Maez, F. (2007). Gas retention in fine-grained pyroclastic flow materials at high temperatures. *Bulletin of Volcanology*, 69(8), 881–901. <https://doi.org/10.1007/s00445-007-0116-7>
- Fisher, R. V., Schmincke, H. U., & Van Bogaard, P. (1983). Origin and emplacement of a pyroclastic flow and surge unit at Laacher See, Germany. *Journal of Volcanology and Geothermal Research*, 17(1–4), 375–392. [https://doi.org/10.1016/0377-0273\(83\)90077-X](https://doi.org/10.1016/0377-0273(83)90077-X)
- 395 Giordano, G., & Cas, R. A. F. (2021). Classification of ignimbrites and their eruptions. *Earth-Science Reviews*, 220(May), 103697. <https://doi.org/10.1016/j.earscirev.2021.103697>
- Giordano, G., De Benedetti, A. A., Diana, A., Diano, G., Esposito, A., Fabbri, M., Gaudio, F., Marasco, F., Mazzini, I., Miceli, M., & others. (2010). Stratigraphy, volcano tectonics and evolution of the Colli Albani volcanic field. In *The Colli Albani Volcano* (pp. 43–97). Geological Society of London. <https://doi.org/10.1144/IAVCEI003.4>
- 400 Giordano, G., and Doronzo, D M. (2017) 'Sedimentation and mobility of PDCs: a reappraisal of ignimbrites' aspect ratio.', *Scientific reports*, 7.1, 4444. doi: 10.1038/s41598-017-04880-6.
- Kennedy, J. F. (1963). The mechanics of dunes and antidunes in erodible-bed channels. *Journal of Fluid Mechanics*, 16(4), 521–544. <https://doi.org/10.1017/S0022112063000975>
- 405 Legros, F., & Kelfoun, K. (2000). On the ability of pyroclastic flows to scale topographic obstacles. *Journal of Volcanology and Geothermal Research*, 98(1–4), 235–241. [https://doi.org/10.1016/S0377-0273\(99\)00184-5](https://doi.org/10.1016/S0377-0273(99)00184-5)
- Lube, G., Breard, E. C., Jones, J., Fullard, L., Dufek, J., Cronin, S. J., & Wang, T. (2019). Generation of air lubrication within pyroclastic density currents. *Nature Geoscience*, 12(5), 381-386. <https://doi.org/10.1038/s41561-019-0338-2>
- 410 Lube, G., Cronin, S. J., Thouret, J. C., & Surono, S. (2011). Kinematic characteristics of pyroclastic density currents at merapi and controls on their avulsion from natural and engineered channels. *Bulletin of the Geological Society of America*, 123(5), 1127–1140. <https://doi.org/10.1130/B30244.1>
- 415 Lube, G., Huppert, H. E., Sparks, R. S. J., & Freundt, A. (2011). Granular column collapses down rough, inclined channels. *Journal of Fluid Mechanics*, 675, 347–368. <https://doi.org/10.1017/jfm.2011.21>
- Marra, F., Karner, D. B., Freda, C., Gaeta, M., & Renne, P. (2009). Large mafic eruptions at Alban Hills Volcanic District (Central Italy): Chronostratigraphy, petrography and eruptive behavior. *Journal of*

- Volcanology and Geothermal Research*, 179(3–4), 217–232.  
420 <https://doi.org/10.1016/j.jvolgeores.2008.11.009>
- Moorhouse, B. L., & White, J. D. L. (2016). Interpreting ambiguous bedforms to distinguish subaerial base surge from subaqueous density current deposits. *The Depositional Record*, 2(2), 173–195.  
<https://doi.org/10.1002/dep2.20>
- 425 Pittari, A. et al. (2006) 'The influence of palaeotopography on facies architecture and pyroclastic flow processes of a lithic-rich ignimbrite in a high gradient setting: the Abrigo Ignimbrite, Tenerife, Canary Islands', *Journal of Volcanology and Geothermal Research*, 152(3-4), 273-315.  
<https://doi.org/10.1016/j.jvolgeores.2005.10.007>.
- 430 Pollock, N. M., Brand, B. D., Rowley, P. J., Sarocchi, D., & Sulpizio, R. (2019). Inferring pyroclastic density current flow conditions using syn-depositional sedimentary structures. *Bulletin of Volcanology*, 81(8). <https://doi.org/10.1007/s00445-019-1303-z>
- Roche, O., Buesch, D. C., and Valentine, G. A. (2016) 'Slow-moving and far-travelled dense pyroclastic flows during the Peach Spring super-eruption', *Nature Communications*, 7(1), 10890.  
<https://doi.org/10.1038/ncomms10890>.
- 435 Rowley, P. J., Kokelaar, P., Menzies, M., & Waltham, D. (2011). Shear-Derived Mixing In Dense Granular Flows. *Journal of Sedimentary Research*, 81(12), 874–884.  
<https://doi.org/10.2110/jsr.2011.72>
- Rowley, P.J., Roche, O., Druitt, T.H. et al. Experimental study of dense pyroclastic density currents using sustained, gas-fluidized granular flows. *Bulletin of Volcanology* 76, 855 (2014).  
<https://doi.org/10.1007/s00445-014-0855-1>
- 440 Schminke, H., Fisher, R. V., & Waters, A. C. (1973). Antidune and chute and pool structures in the base surge deposits of the Laacher See area, Germany. *Sedimentology*, 20(4), 553–574.  
<https://doi.org/10.1111/j.1365-3091.1973.tb01632.x>
- 445 Shimizu, H. A., Koyaguchi, T., & Suzuki, Y. J. (2019). The run-out distance of large-scale pyroclastic density currents: A two-layer depth-averaged model. *Journal of Volcanology and Geothermal Research*, 381, 168–184. <https://doi.org/10.1016/j.jvolgeores.2019.03.013>
- Smith, G. M., Williams, R., Rowley, P. J., & Parsons, D. R. (2018). Investigation of variable aeration of monodisperse mixtures: implications for pyroclastic density currents. *Bulletin of Volcanology*, 80(8). <https://doi.org/10.1007/s00445-018-1241-1>
- 450 Smith, G., Rowley, P., Williams, R., Giordano, G., Trolese, M., Silleni, A., Parsons, D. R. D. R., & Capon, S. (2020). A bedform phase diagram for dense granular currents. *Nature Communications*, 11(1), 1–11. <https://doi.org/10.1038/s41467-020-16657-z>
- Smith, N. J., & Kokelaar, B. P. (2013). Proximal record of the 273 ka Poris caldera-forming eruption, Las Cañadas, Tenerife. *Bulletin of Volcanology*, 75(11), 1–21. <https://doi.org/10.1007/s00445-013-0768-4>
- 455 Sohn, Y. K., & Chough, S. K. (1993). The Udo tuff cone, Cheju Island, South Korea: transformation of pyroclastic fall into debris fall and grain flow on a steep volcanic cone slope. *Sedimentology*, 40(4), 769–786. <https://doi.org/10.1111/j.1365-3091.1993.tb01359.x>
- 460 Sparks, R. S. J. (1976). Grain size variations in ignimbrites and implications for the transport of pyroclastic flows. *Sedimentology*, 23(2), 147–188. <https://doi.org/10.1111/j.1365-3091.1976.tb00045.x>
- Sulpizio, R., Dellino, P., Doronzo, D. M., & Sarocchi, D. (2014). Pyroclastic density currents: State of the art and perspectives. *Journal of Volcanology and Geothermal Research*, 283, 36–65.  
<https://doi.org/10.1016/j.jvolgeores.2014.06.014>
- Trolese, M., Giordano, G., Cifelli, F., Winkler, A., & Mattei, M. (2017). Forced transport of thermal

- 465 energy in magmatic and phreatomagmatic large volume ignimbrites: Paleomagnetic evidence  
from the Colli Albani volcano, Italy. *Earth and Planetary Science Letters*, 478, 179–191.  
<https://doi.org/10.1016/j.epsl.2017.09.004>
- Wilson, C. J. N. (1980). The role of fluidization in the emplacement of pyroclastic clasts: An  
experimental approach. *Journal of Volcanology and Geothermal Research*, 8(2–4), 231–249.  
470 [https://doi.org/10.1016/0377-0273\(80\)90106-7](https://doi.org/10.1016/0377-0273(80)90106-7)
- Wilson, G., Wilson, T. M., Deligne, N. I., & Cole, J. W. (2014). Volcanic hazard impacts to critical  
infrastructure: A review. *Journal of Volcanology and Geothermal Research*, 286, 148–182.  
<https://doi.org/10.1016/j.jvolgeores.2014.08.030>

475